Available online at www.sciencedirect.com
ScienceDirect
Bioorganic & Medicinal Chemistry 16 (2008) 3049–3058
Bioorganic & Medicinal Chemistry

Docking analyses on human muscarinic receptors: Unveiling the subtypes peculiarities in agonists binding

Giulio Vistoli,[a,*] Alessandro Pedretti,[a] Silvia Dei,[b] Serena Scapecchi,[b] Cristina Marconi[a] and Maria Novella Romanelli[b]

[a]*Istituto di Chimica Farmaceutica e Tossicologica "Pietro Pratesi", Università di Milano, Via Mangiagalli, 25 I-20133 Milano, Italy*
[b]*Dipartimento di Scienze Farmaceutiche, Università di Firenze, via U. Schiff 6, 50019 Sesto Fiorentino (FI), Italy*

Received 22 June 2007; revised 13 December 2007; accepted 18 December 2007
Available online 7 January 2008

Abstract—The study presents a docking analysis for the interaction capabilities of some muscarinic receptors (i.e., M_1, M_2, and M_5) whose full-length models were previously generated by us. In detail, the docking simulations involved a dataset of 30 agonists, taken from the literature, including a first series of oxathiolane/dioxolane congeners and a second subset of more heterogeneous ligands. The obtained results unveil that it is possible to discriminate among the binding modes of considered muscarinic receptors, developing specific interaction patterns which are significantly different for the arrangement of both polar and hydrophobic interactions. Thus, the M_1 subtype possesses the widest binding site, while the M_2 receptor is characterized by a large but asymmetric region that accommodates the ligand's ammonium head and finally the M_5 binding site is quite similar to that of M_2 subtype being univocally characterized by a second aspartate residue which interacts with the ammonium head. The significant correlations between docking scores and affinity values afford an encouraging validation for the reported binding modes and confirm the key role of molecular flexibility in the ligand recognition of muscarinic receptors.

1. Introduction

The muscarinic receptor family (mAChR), whose activation mediates the metabotropic actions of acetylcholine, belongs to class I of G-protein coupled receptors (GPCRs) and includes five distinct subtypes, denoted as muscarinic M_1–M_5 receptors.[1–3] Muscarinic receptors are widely distributed throughout the human body and control distinct physiological functions according to location and receptor subtype. They have been cloned from several species and exhibit a marked sequence homology among subtypes and across species.[4] Based on their activation mechanism, these receptors can be divided in two main classes. The odd-numbered receptors couple to G_q/G_{11} proteins and induce the hydrolysis of phosphoinositide lipids by several forms of phospholipase, while M_2 and M_4 subtypes are linked to G_i/G_0 proteins and inhibit the adenylyl cyclase.[5]

The marked similarity among the muscarinic subtypes and, in particular, in their ligand binding sites can explain the historical difficulty in the identification of subtype-selective compounds, even though there is still a demand for really selective ligands, which could be clinically useful in treating, for example, Alzheimer's disease, pain, schizophrenia, and intestinal hypomotility.[6]

A comparison of the amino acidic sequence for the five human mAChRs shows a vast homology among them, with many residues conserved in all subtypes being significantly abundant in the seven transmembrane helices. Interestingly, some residues are identical in M_1, M_3, and M_5 subtypes being replaced by a different residue, but identical in M_2 and M_4 subtypes. Finally the large third cytoplasmatic loops show virtually no homology among the mAChR subtypes (except for a short Ser/Thr-rich region).[7]

Nevertheless, it is well known that even single residue differences in GPCR sequence can afford significant differences in binding site architecture and, hence, in ligand affinities.[8] Therefore, a comparative analysis of the critical interactions in mAChR binding sites can give

Keywords: Muscarinic receptors; Molecular docking; Muscarinic agonists; Subtype-selectivity.
* Corresponding author. Tel.: +39 02 50319349; fax: +39 02 50319359; e-mail: giulio.vistoli@unimi.it

0968-0896/$ - see front matter © 2007 Elsevier Ltd. All rights reserved.
doi:10.1016/j.bmc.2007.12.036

new insights to design subtype-selective muscarinic ligands and to understand the ligand recognition at an atomic level.

Such an analysis is strongly supported by mutagenesis studies that have unraveled the key residues involved in ligand binding. In all mAChRs, an ion pair between the acetylcholine ammonium head and a conserved aspartate residue in TM3 (Asp105 in M_1, Asp103 in M_2, Asp147 in M_3, Asp112 in M_4, and Asp110 in M_5) plays a key role in the ligand–receptor complex stabilization.[9] The electrostatic interaction is reinforced by a cluster of six aromatic residues conserved across the five muscarinic receptors but not in other GPCRs. For example, mutagenesis experiments have shown the pivotal role of two tryptophan and four tyrosine residues in M_3 subtype (Trp143, Tyr148, Trp503, Tyr506, Tyr529, and Tyr533).[10] The pattern of residues interacting with the acetylcholine ester group is more heterogeneous even if it seems characterized by a conserved threonine residue in TM5, which presumably stabilizes H-bonds with the ester moiety.[11]

The experimental crystal structure of bovine rhodopsin laid the way for the homology modeling of full-length G protein coupled receptors. In recent years, several reliable GPCR homology models appeared in the literature and were successfully used for virtual screening and ligand optimization.[12,13] On these grounds, in a previous study we have generated full-length reliable models for all muscarinic receptor subtypes exploring their ability to interact with acetylcholine.[14,15]

The present study reports an exhaustive docking analysis, in which we considered a representative dataset of 30 muscarinic agonists taken from the literature (as

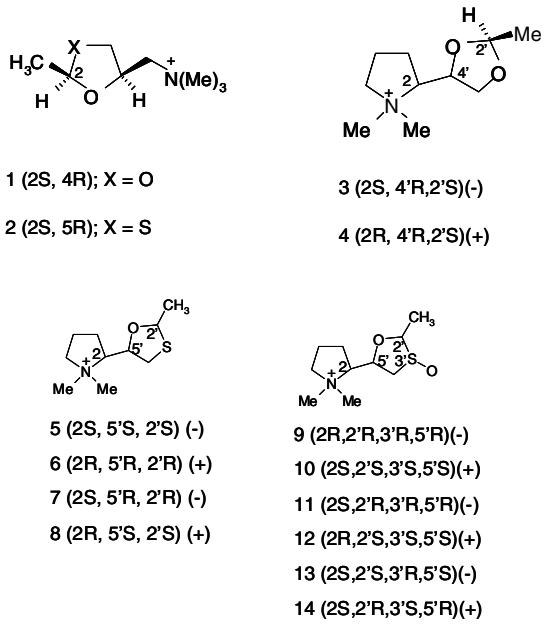

Chart 1. The subset of dioxolane and oxathiolane derivatives.

Table 1. Binding affinities (as expressed by p*K* values) and docking scores (i.e., ChemScores, as computed by Fred software and expressed in kcal/mol) for the docked muscarinic agonists

Compound	*I*(Flex)	pKM_1	Score M_1	pKM_2	Score M_2	pKM_5	Score M_5	Ref.
1	0	4.96	−15.58	5.92	−15.8	4.66	−19.65	35
2	0	4.96	−15.64	5.68	−15.43	4.88	−20.03	35
3	1	4.67	−18	5.77	−23.1	4.64	−23.21	35
4	1	4.28	−17.23	5.3	−21.4	4.28	−21.58	35
5	1	5.08	−18.96	6.17	−24.01	4.99	−24.17	35
6	1	4.72	−17.54	5.28	−22.9	4.61	−23.74	35
7	1	4.85	−18.53	5.45	−23.12	4.63	−23.77	35
8	1	5.23	−19.23	5.85	−23.81	4.97	−24.28	35
9	1	n.a.		5.03	−21.99	n.a.		36
10	1	n.a.		4.11	−20.99	n.a.		36
11	*1*	*4.03*	*−17.32*	*4.81*	*−22.15*	*4.47*	*−22.18*	*36*
12	*1*	*n.a.*		*4.09*	*−20.67*	*4.24*	*−21.25*	*36*
13	1	n.a.		4.54	−21.63	n.a.		36
14	1	n.a.		4.29	−20.79	n.a.		36
15 (muscarine)	0	4.74	−15.66	6.31	−18.76	n.a.		37
16 (arecoline)	0	4.53	−14.25	5.61	−11.61	4.25	−14.71	38
17 (milameline)	0	5.25	−14.32	6	−13.44	5.5	−16.89	24
18 (xanomeline)	0	8.1	−22.87	7.93	−24.44	7.82	−28.95	42
19 (oxotremorine)	0	8.95	−24.19	6.49	−19.08	n.a.		39
20 (oxotremorine-M)	0	4.69	−17.32	6.97	−17.89	n.a.		39
21	*0*	*6.92*	*−17.53*	*6.99*	*−17.16*	*7.29*	*−18.83*	*44*
22	*0*	*7.04*	*−19.25*	*8.44*	*−20.49*	*8.21*	*−28.98*	*44*
23 (pilocarpine)	0	5.18	−16.77	4.92	−13.97	4.99	−15.93	40
24 (*S*-aceclidine)	0	n.a.		6.21	−12.88	n.a.		41
25 (*R*-aceclidine)	0	n.a.		5.65	−12.33	n.a.		41
26 (sabcomeline)	0	6.64	−15.92	6.69	−14.18	n.a.		42
27	*0*	*4.67*	*−14.79*	*8.58*	*−21.7*	*n.a.*		*43*
28	*0*	*3.55*	*−13.89*	*5.56*	*−12.7*	*n.a.*		*43*
29 (carbachol)	0	4.92	−11.02	5.88	−12.99	5.37	−17.09	38
30	0	5.08	−14.76	4.43	−14.91	5.43	−17.76	29

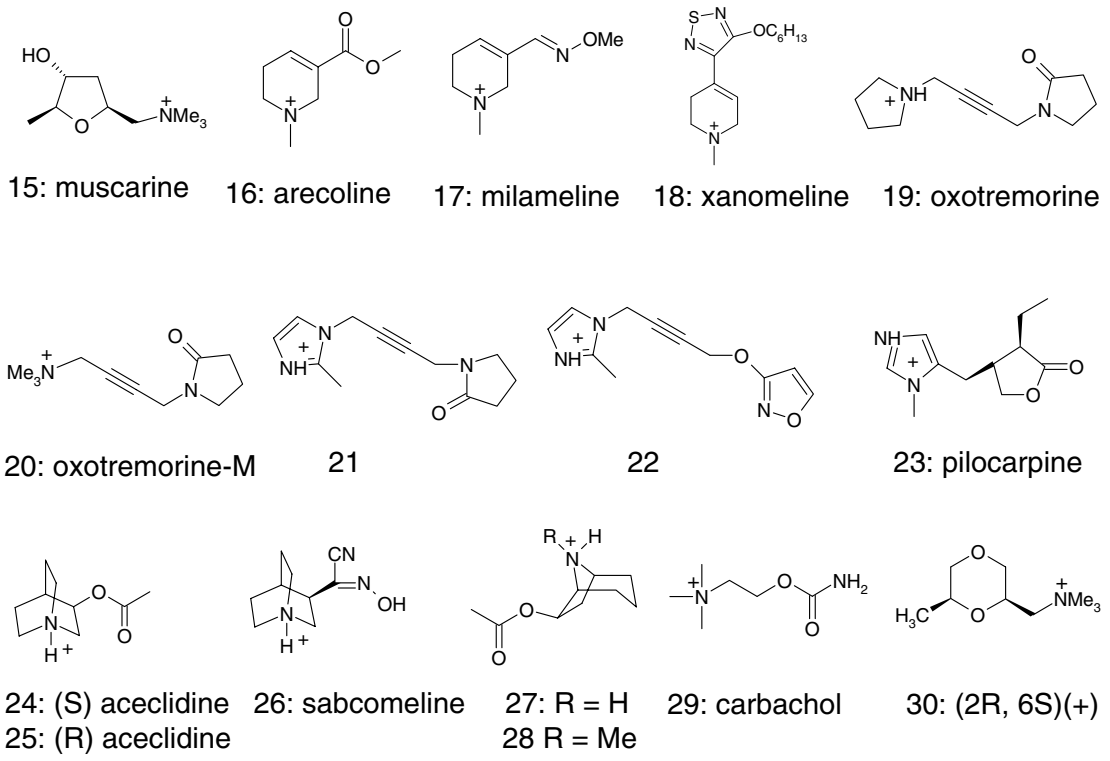

Chart 2. The second and more heterogeneous subset of docked muscarinic agonists.

compiled in Table 1, Charts 1 and 2). It is worth noting that the choice and the total number of considered ligands were severely limited by the marked scarcity of comparable binding data for known muscarinic agonists (especially for M_5 subtype). Nonetheless, the obtained results allow the binding sites peculiarities to be unveiled, deriving subtype-selective interaction patterns which, hopefully, could be exploited to design novel muscarinic ligands with an improved selectivity profile.

Given the mentioned similarity among muscarinic receptors, the docking calculations were focused on M_1, M_2, and M_5 subtypes only. The study has been subdivided in three phases: first, the most numerous series of congeners (namely the dioxolane/oxathiolane derivatives **1–14**, Chart 1) was used to generate reliable interaction patterns for each investigated subtype. Then, such binding modes were verified and refined by docking the remaining and more heterogeneous ligands in the dataset (**15–30**, Chart 2). Finally, the obtained results were assessed by correlating docking scores versus affinity values and, then, converted into subtype-selective interaction schemes which shed light on the key differences among the muscarinic receptors.

2. Results

2.1. Muscarinic M_1 subtype

Figure 1 illustrates the main interactions realized by oxathiolane and dioxolane derivatives (**1–14**) with the M_1 subtype. The charged group interacts with Asp105, Ser109, and a set of aromatic residues, which reinforce the ionic interactions (i.e., Tyr106, Trp157, Phe197, Trp378, and Tyr 381). The oxygen atom in 1′ interacts with Thr192, while the heteroatom in 3′ (S or O) may contact Asn382, even if its role seems less important than that of Thr192 as confirmed by mutational analyses.[16] The methyl group in C2′ realizes apolar contacts with Leu386 and Ala193. Globally, such results appear in agreement with both mutagenesis studies[17–19] and the recent models proposed by Goddard and co-workers[20] and Hulme and co-workers.[21] Specifically, docking results are consistent with recent mutational analysis which suggested that synthetic agonists do not realize specific polar interactions with TM3 residues (except for Asp105).[22]

In the light of such pivotal interactions and considering the binding data of these congeners (**1–14**), it is possible to draw some relevant considerations. The ionic interaction involving the charged nitrogen atom is clearly mandatory being realized by all docked ligands. Since the H-bond with Thr192 is more relevant than that with Asn382,[16] it comes as no surprise that the oxathiolane derivatives arrange always the oxygen atom close to Thr192 to optimize such an interaction. The most affinitive compounds (i.e., **5** and **8**) have the methyl group in C2′ over the oxathiolane plane to maximize the hydrophobic contacts with Leu386 and Ala193. This finding confirms the role of apolar interactions in M_1 subtype and underlines the relevance of C2′ configuration in such congeners. This is also in line with mutagenesis results which have unveiled that the mutation of Ala193 is even more detrimental to agonist affinity than

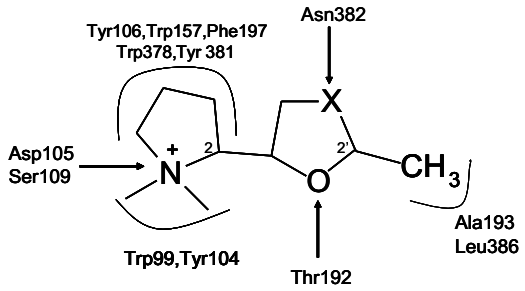

Figure 1. Bi-dimensional scheme of the main interactions stabilizing the agonist binding in M_1 subtype (legend: the arrows indicate polar interactions, namely ion pairs and H-bonds, and the lines represent hydrophobic contacts).

that of Thr192.[23] Conversely, the configuration of C2 and C5′ should not play a significant role, probably because such ligands are always able to realize the polar contacts with both Asp105 and Thr192 due to the intramolecular interaction between ammonium group and oxygen atom which constrains their conformation irrespective of the configuration of C2 and C5′.

The greater affinity of oxathiolane derivatives, (**5–8**) if compared to dioxolanes (**3–4**), emphasizes the beneficial role of the sulfur atom which reinforces the hydrophobic contacts with apolar residues surrounding the ligand. Such an effect is well understandable here due to the modest role of H-bond with Asn382.

Hence, the loss of affinity of the sulfoxide derivatives (**9–14**) toward the M_1 subtype can be explained considering that such a function cannot add extra polar interactions, given the scarce relevance of H-bond with Asn382, but vastly reduces the hydrophobic contacts of the sulfur atom. Probably, the sulfoxide function could interact with Thr192, but such a contact would require a ligand overturning into the binding site with a consequent weakening of the interactions involving ammonium head and C2′ methyl group. Thus, it is not surprising that the sole sulfoxide derivative with a detectable affinity toward M_1 subtype (i.e., **11**) shows a C2′ configuration, which is inverted in respect to the most active oxathiolane derivatives. This permits the interaction between sulfoxide and Thr192 even conserving the apolar contacts with Leu386 and Ala193.

The interaction topography derived from the congeners (**1–14**) into M_1 binding site finds relevant confirmations when analyzing the docking results for the more heterogeneous agonists in the dataset (**15–30**), allowing to further detail the interaction capabilities of M_1 subtype. While arecoline (**16**), milameline[24] (**17**), sabcomeline (**26**, whose nitrile group also interacts with Thr189), and carbachol (**29**, where the carbamoyl group also contacts Thr189) bind the receptor with a binding mode nearly identical to that previously described, muscarine (**15**) and pilocarpine (**23**) interact with a quite opposite interaction pattern, since they realize a strong H-bond with Asn382 but do not interact with Thr192, suggesting that such H-bonds are rather interchangeable.

Also the most affinitive derivatives in the dataset (namely xanomeline, **18**, and oxotremorine, **19**) cannot realize both H-bonds, but interact only with Thr192. In detail, the remarkable affinity of xanomeline may be ascribed to hexoxy chain, which realizes apolar contacts with Ala193, Phe197, Tyr198, and Leu386 (as seen in Fig. 2), while the high affinity of oxotremorine can be explained considering that the pyrrolidinone ring interacts also with Tyr106 and Tyr381.

Noticeably, **22** is the sole derivative, which realizes both H-bonds (namely, Thr192 with ether function and Asn382 with dihydroisoxazol ring), and it shows a good but not exceptional affinity, signifying that such interactions are surely beneficial but they can be replaced by more effective contacts (as seen for xanomeline and oxotremorine).

2.2. Muscarinic M_2 subtype

Figure 3 shows the main interactions stabilizing the complexes between the congeners (**1–14**) and the M_2 subtype. Thus, the charged nitrogen atom interacts with Asp 103 in TM3 plus a set of aromatic residues which reinforce the ionic interaction (e.g., Tyr80, Trp99, Tyr104, and Tyr177). The oxygen atom in 1′ interacts with Tyr104 and, minor extent, with Thr434. The heteroatom in 3′ (S or O) interacts with Ser107 and, minor extent, with Tyr403 whose role in agonist interaction has been confirmed by mutagenesis.[25] The N-linked methyl groups should be inserted in a pocket lined by Trp99 and Tyr104. Finally the methyl group in C2′ can realize apolar contacts with either Val407 or Tyr403, even if the greater richness of apolar residues in the M_2 binding site renders the ligand affinity less dependent on the C2′ configuration (if compared to M_1 subtype). The threonine residues in TM5 (i.e., Thr187 and Thr190) appear not clearly involved in ligand interaction as also proven by both experimental data[26] and the models of Holtje and co-workers,[27] which suggest that such threonine residues may be involved in the interaction with antagonists, as proposed for (*S*)-scopolamine.

When comparing such interactions with those realized by M_1 subtype, it emerges as main difference that in

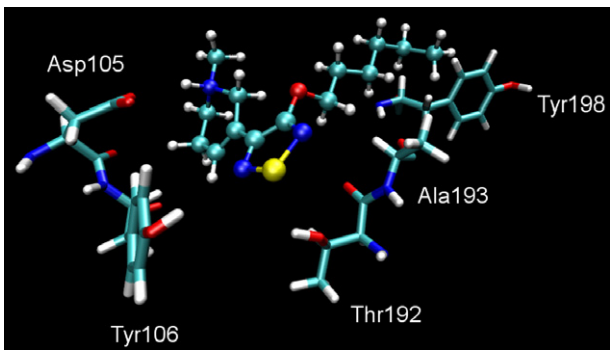

Figure 2. Main interactions stabilizing the complex between xanomeline (**18**) and M_1 subtype. Notice the apolar contacts which the hexoxy chain realizes with Ala193, Tyr198 plus other apolar residues not displayed for clarity.

the M_2 receptor both heteroatoms are involved in significant H-bond interactions, while in M_1 subtype only the oxygen atom in 1′ is involved in a strong H-bond whereas the interaction with Asn382 is uncertain and however weak.

In the light of the described interactions and considering the affinity values of these congeners (**1–14**), it is possible to derive some interesting considerations. The ionic interaction involving the charged nitrogen atom is mandatory being realized by all docked ligands. The key role of both H-bonds (with Tyr104 and Ser107) is confirmed by the fact that the most affinitive compounds (i.e., **1** and **5**) are able to realize both H-bonds. The most affinitive congeners are characterized by the same C5′ configuration and this modifies the M_2 affinity rank of considered oxathiolane derivatives if compared to M_1 affinities (i.e., **8** > **5** > **7** > **6** in M_1 and **5** > **8** > **7** > **6** in M_2). This fact is well understandable since the C5′ configuration influences both the position of heteroatoms optimizing the H-bonds and the arrangement of pyrrolidine ring allowing the hydrophobic contacts between methyl groups and Trp99/Tyr104. Again, the greater affinity of oxathiolane derivatives (if compared to dioxolanes) emphasizes the dual role of the sulfur atom, which realizes the H-bond with Ser107 even assuring an optimal lipophilicity to maximize the apolar contacts.

The maximal affinity of **5** can be interpreted considering that such ligand is able to realize almost all described interactions (as seen in Fig. 4). Moreover, the differences between **5** and the other oxathiolane derivatives can be exploited to derive the specific role of each interaction. Thus, **6** realizes the same interactions of **5** apart from the arrangement of methyl groups which are exposed toward Thr434 and Pro437 instead of Trp99 and Tyr104. Again, **8** realizes the same interactions but the H-bond between the O atom in 1′ and Tyr104 is weakened by the shielding effect of methyl group in C2′. Similarly, **7** realizes the same interactions except for the H-bond between the S atom in 3′ and Tyr104, which is virtually lost by the shielding effect of methyl group in C2′.

Overall, such analysis emphasizes the relevance of a suitable arrangement of ammonium methyl groups. Indeed, the lowest affinitive isomer (i.e., **6**) is unable to correctly arrange the methyl groups, while the loss (or the weakening) of an H-bond induces a minor decrease in binding affinities, probably as the H-bonds are somewhat exchangeable (as already seen in M_1 subtype). The key role of N-linked methyl groups can be explained considering that an unsuitable arrangement of such groups can: (1) reduce the hydrophobic contacts; (2) weaken the ion pair with Asp103, and (3) distort the fine architecture of the M_2 binding site.

The marked affinity of sulfoxide derivatives emphasizes the relevance of H-bonding in M_2. In particular, the affinity of **9** is understandable in terms of reinforced H-bonds which sulfoxide function can realize with Ser107, while the difference between **9** and **10** confirms the relevance of a correct pose of ammonium methyl groups. Indeed, the two enantiomers realize nearly the same interactions and the sole difference is that the eutomer exposes the methyl groups toward Trp99 and Tyr104, whereas the diastomer toward Thr434 and Pro437. Curiously, the difference between **9** and **10** in the sulfoxide derivatives is nearly identical to that between **5** and **6** in the oxathiolane compounds, indicating that an unfit arrangement of methyl group induces a similar detrimental effect on ligand affinity.

The more relevant role of the H-bond with Tyr104 (if compared to that with Ser107) may be suggested by the affinity difference between **11** and **12**. Indeed, the main difference between the corresponding complexes is that in the first the sulfoxide function interacts with Ser107 and the H-bond with Tyr104 is virtually lost, whereas in the eutomer the sulfoxide function interacts with Tyr104 and the H-bond with Ser107 is all but lost.

The docking results obtained by the second heterogeneous part of dataset (**15–30**) afford relevant validations for the described interactions pattern. Thus, the tropane derivatives (**27–28**) confirm the pivotal role of the hydrophobic contacts that the ammonium methyl groups realize with Trp99/Tyr104 as proven by the significant activity and selectivity of **27** which properly inserts the

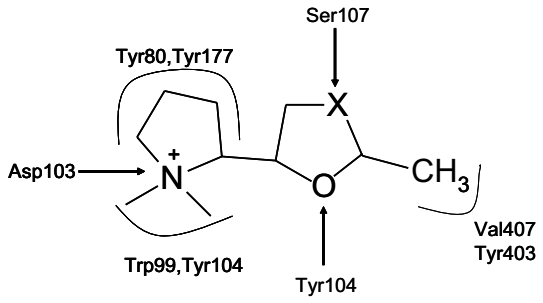

Figure 3. Bi-dimensional scheme of the main interactions stabilizing the agonist binding in M_2 subtype (legend: the arrows indicate polar interactions, namely ion pairs and H-bonds, and the lines represent hydrophobic contacts).

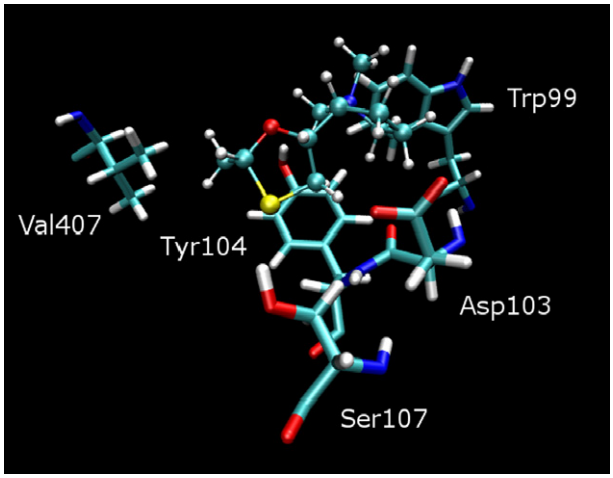

Figure 4. Main interactions stabilizing the complex between **5** and M_2 subtype.

nortropane scaffold in such apolar subpocket. Conversely, the markedly lower affinity of **28** may be ascribed to *N*-methyl group which clashes against Pro437 distorting the architecture of the M_2 binding site. The different role of apolar contacts realized with Trp99/Tyr104 or with Pro437 is in line with previous COMFA studies which emphasized the key relevance of steric contribution for the agonist affinities revealing that the N-linked alkyl substituents can elicit contrasting effects depending on their arrangement.[28] Similarly, aceclidine isomers (**24–25**) and sabcomeline (**26**) realize the mentioned H-bonds with Tyr104 and Ser107 but fail to suitably accommodate the azabicyclic moiety near to Trp99/Tyr104.

Furthermore, the oxotremorine derivatives (**19–22**) confirm the relevance of H-bonds involving Tyr104 and Ser107. Such compounds are all able to realize both interactions and the similar affinity of oxotremorine (**19**) and **21** suggests that the methyl-imidazole moiety can replace the pyrrolidine ring conserving both the ionic and the hydrophobic interactions. Conversely, the greater affinity of **22** can be explained considering that, while the other oxotremorine analogs (**19–21**) are conformationally constrained by intramolecular interaction between carbonyl group and ammonium head, which hampers their contacts with the receptor, all moieties of **22** are fully accessible to suitably interact with M_2 receptor and the carbon skeleton of isoxazolinyl ring can successfully contact Val407 and Phe195.

2.3. Muscarinic M_5 subtype

Figure 5 depicts the main interactions stabilizing the complexes between considered congeners (**1–14**) and the M_5 subtype. The charged nitrogen atom interacts with both Asp110 in TM3 and Asp181 in the second extracellular loop (EL2) plus a set of aromatic residues which reinforce the ionic interactions (Tyr111, Trp455, Tyr458, and Tyr481). The oxygen atom in 1′ forms a clear H-bond with Ser114, while the heteroatom in 3′ (S or O) weakly interacts with both Tyr111 and Cys383. Finally, the methyl group in C2′ is inserted in a pocket lined by Trp455 and Phe202.

When analyzing the affinity values of such congeners (**1–14**) at M_5 subtype, it is evident that their variability is particularly reduced probably because the docked agonists realize a very similar interactions pattern and, indeed, the main difference involves the methyl group in 2′ that only in the most affinitive derivatives (i.e., **2**, **5**, and **8**) contact Trp455 and Phe202. The affinity differences between dioxolane (**3–4**) and oxathiolane (**5–8**) derivatives confirm that a lipophilic group in 3 is more beneficial than a strong H-bond acceptor, underlining the modest role of H-bond with Tyr111/Cys383.

The poor affinity of sulfoxide derivatives (**9–14**) confirms the different roles of H-bonds: indeed, the affinity loss of many sulfoxide derivatives can be explained considering that they lose the H-bond with Ser114, even realizing a reinforced interaction with Tyr111/Cys383. And indeed, the derivatives which are affinitive at M_5 subtype are able to arrange the sulfoxide near to Ser114 (as in the case of **11** and **12**).

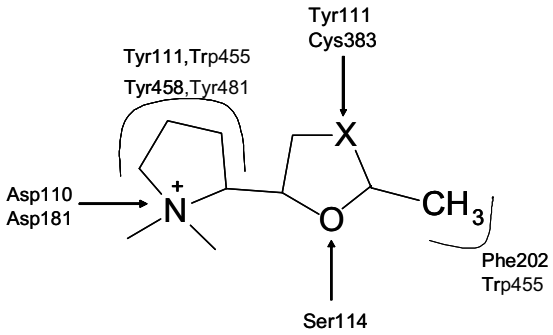

Figure 5. Bi-dimensional scheme of the main interactions stabilizing the agonist binding in M_5 subtype (legend: the arrows indicate polar interactions, namely ion pairs and H-bonds, and the lines represent hydrophobic contacts).

Although the binding data on M_5 subtype are rather rare in the literature, the docking results of the second heterogeneous agonists set (**15–30**) permit to confirm the interaction pattern as previously depicted. The significant affinity of **21** and **22** is well understandable considering that the methyl-imidazole moiety increases the delocalization of positive charge maximizing the ionic interactions with both Asp110 and Asp181 (as seen in Fig. 6). Moreover, the remarkable affinity of xanomeline (**18**) confirms the key role of hydrophobic interactions in M_5 subtype since the hexoxy chain contacts a set of apolar residues (e.g., Tyr111, Phe202, Trp455, and Tyr458). Finally arecoline (**16**), milameline (**17**), pilocapine (**23**), charbachol (**29**), and **30**[29] bind the receptor with an interaction pattern very similar to that previously described for the congeners **1–14**, thus justifying their intermediate affinity.

3. Discussion

3.1. Docking scores predictivity

As detailed under Methods, all docking functions, computed by Fred software, were tentatively exploited to predict the affinity data, unveiling that ChemScore affords the best correlations between docking scores and affinity values. This finding is well interpretable remembering that such a score considers both polar and hydrophobic contacts accounting also for steric fitting between ligand and receptor. Hence, the docking scores compiled in this study (as seen in Table 1) refer to the ChemScore function only.

A bird's eye analysis of docking results (as compiled in Table 1) reveals that the bicyclic oxathiolane/dioxolane derivatives show reduced affinities, although they possess remarkable docking scores and this discrepancy is palpable in all considered subtypes. Since in a previous study[30] we have showed that the muscarinic receptors are markedly flexible and able to recognize more acetylcholine conformers, such divergent results may

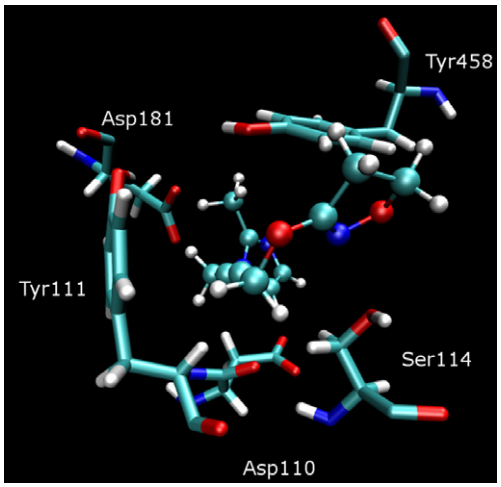

Figure 6. Main interactions stabilizing the complex between **22** and M_5 subtype. Notice the isoxazolinyl ring which realizes H-bonds with both Ser114 and Tyr458.

suggest that very rigid compounds are not able to parallel the receptor mobility, thus decreasing their affinities even when they are successfully accommodated in the complementary binding sites. In detail, the compounds which pay such kind of penalty are those being less flexible than acetylcholine, namely with only one rotatable bond.

On these bases, we introduced in the affinity versus docking score relationships a constitutional binary descriptor (I_{flex}) which identifies the ligands which are more rigid than acetylcholine. More in detail, such a descriptor is equal to 1 for compounds with only one rotatable bond (i.e., derivatives **3–14**) and 0 otherwise (as seen in Table 1). Clearly, the discrepancy among the docking scores can be also resolved by deriving two separate correlative equations (namely the first for rigid compounds only and the latter for the other ligands, as reported in Table 2), but the introduction of such a binary descriptor allows to develop single correlative equations which are predictive for all ligands irrespective of their flexibility.

Table 2 reports the predictive equations obtained correlating docking scores versus affinity data with and without the I_{flex} descriptor as well as the correlations obtained by considering separately the flexible ligands and the rigid congeners (**3–14**). One can note that in all subtypes the introduction of I_{flex} descriptor vastly enhances the predictive power of the relations which consider all ligands together. What is more, Table 2 emphasizes that it is possible to develop predictive relationships for all considered subtypes.

Although the mentioned discrepancy renders the global correlations without I_{flex} statistically modest, the predictive power of the ChemScore values becomes evident when analyzing the two subsets separately (as seen in Table 2). In all subtypes, the relations for rigid congeners (**3–14**) perform better than those for flexible ligands and this is easily interpretable in terms of structural homogeneity of the rigid oxathiolane/dioxolane derivatives. However, also the more flexible and heterogeneous ligands afford significant relationships which can be exploited to rationalize and predict the affinity of novel muscarinic agonists.

Globally, the significant predictive power of the correlations compiled in Table 2 affords an encouraging validation for the described docking results, and, ultimately, for the previously generated muscarinic models, and suggests that they can be successfully used to assist the design of improved muscarinic agonists.

3.2. Subtype-selective interaction pattern

The reported results can be also used, in this last step, to compare the arrangement of key residues involved in ligand recognition with the aim to shed light on the critical differences among the considered subtypes.

Figure 7 show that in all considered subtypes the residues which can realize polar interaction with agonists can be placed on the vertices of a triangle which characterizes the binding site architecture. Hence, the analysis of geometric features of the so obtained triangles can be

Table 2. Relationships between docking scores and affinities for the three considered muscarinic subtypes

Muscarinic receptor	Relationship	Statistical parameters
M_1		
Without I_{flex}	$pKM_1 = -0.3121$ Score M1 + 0.0489	$N = 23$; $r^2 = 0.47$; $s = 0.99$; $F = 18.79$
With I_{flex}	$pKM_1 = -0.3806$ Score M1 − 1.5627 I_{flex} − 0.6388	$N = 23$; $r^2 = 0.77$; $s = 0.66$; $F = 33.05$
Only rigid congeners	$pKM_1 = -0.4811$ Score M1 − 4.0204	$N = 7$; $r^2 = 0.84$; $s = 0.17$; $F = 38.87$
Only flexible ligands	$pKM_1 = -0.3783$ Score M1 − 0.5996	$N = 16$; $r^2 = 0.74$; $s = 0.77$; $F = 25.82$
M_2		
Without I_{flex}	$pKM_2 = -0.1010$ Score M2 + 5.6437	$N = 30$; $r^2 = 0.10$; $s = 1.17$; $F = 1.04$
With I_{flex}	$pKM_2 = -0.2598$ Score M2 − 2.8790 I_{flex}+ 2.1659	$N = 30$; $r^2 = 0.73$; $s = 0.62$; $F = 36.28$
Only rigid congeners	$pKM_2 = -0.5585$ Score M2 − 7.3492	$N = 12$; $r^2 = 0.86$; $s = 0.27$; $F = 60.32$
Only flexible ligands	$pKM_2 = -0.2400$ Score M2 + 2.4844	$N = 18$; $r^2 = 0.68$; $s = 0.72$; $F = 25.92$
M_5		
Without I_{flex}	$pKM_5 = -0.1333$ Score M5 + 2.4536	$N = 18$; $r^2 = 0.20$; $s = 1.12$; $F = 4.03$
With I_{flex}	$pKM_5 = -0.2297$ Score M5 − 1.9576 I_{flex}+ 1.2735	$N = 18$; $r^2 = 0.78$; $s = 0.61$; $F = 26.03$
Only rigid congeners	$pKM_5 = -0.2172$ Score M5 − 0.3975	$N = 8$; $r^2 = 0.87$; $s = 0.11$; $F = 39.44$
Only flexible ligands	$pKM_5 = -0.2302$ Score M5 + 1.2627	$N = 10$; $r^2 = 0.69$; $s = 0.83$; $F = 17.62$

a first relevant approach to differentiate the binding modes of the considered muscarinic subtypes.

Thus, Figure 7A shows that the three polar residues involved in ligand recognition in M_1 subtype (namely, Asp105, Thr192, and Asn382) lie on the vertices of an equilateral triangle with the sides about equal to 9.75 Å. The marked distance among the considered residues can explain why: (1) most docked ligands are able to realize only one H-bond, and (2) the acetylcholine interacts with M_1 subtype mainly assuming full-extended conformations[30] implying that a ligand has to mimic such extended geometries to suitably interact with M_1 subtype.

Conversely, Figure 7B suggests that the three key residues implicated in ligand binding for M_2 subtype (namely, Asp103, Tyr104, and Ser107) lie on the vertex of a smaller isosceles triangle in which the shortest side (i.e., Asp103–Ser107) is about equal to 5 Å and the other two sides equate about 8.5 Å. The greater closeness among the considered polar residues can explain why (1) almost all docked agonists are able to realize both H-bonds; (2) acetylcholine interacts with M_2 subtype largely assuming **gt** conformation as experimentally demonstrated by coupling constants values and nuclear Overhauser effect spectroscopy data.[31]

Finally, Figure 7C shows that the interaction scheme of M_5 subtype is quite identical to that of M_2 subtype both for residue composition (i.e., Asp110, Tyr111, and Ser114) and geometric features of isosceles triangle (one side about equal to 5.5 Å and the other two equal to 8.5 Å). The main difference between M_2 and M_5 subtypes concerns the second aspartate residue (Asp181) which univocally characterizes the M_5 binding site. Consequently, the four polar residues of M_5 subtype can also define a quadrilateral with two short sides (about 5 Å) between Asp110 and Ser114 and between Asp181 and Tyr111 and two longer sides (about 8.5 Å) between Asp110 and Tyr111 and between Asp181 and Ser114.

The different distances between the pivotal polar residues in each subtype reflect in the different volumes of binding sites as computed by CASTp software.[32,33] Specifically, the volume of M_1 binding site (as reported in Table 3) is more than twice if compared to volumes of binding sites in M_2 and M_5 subtypes which have a nearly identical volume.

While the residues contacting the ester function in M_2 and M_5 subtypes belong to TM3 and are sequentially close to aspartate residue, in M_1 subtype the residues which realize H-bond belong to TM5 and TM6 and the polar residues of TM3, close to Asp105 (e.g., Tyr106, Ser109, and Ser112), do not contact the ester moiety but, at most, reinforce the ion-pair between aspartate and ammonium group. This observation is in agreement with recent mutagenesis studies[22] and suggests that the insertion of an H-bond acceptor group very close to ammonium head may improve the ligand affinity toward the M_1 subtype.

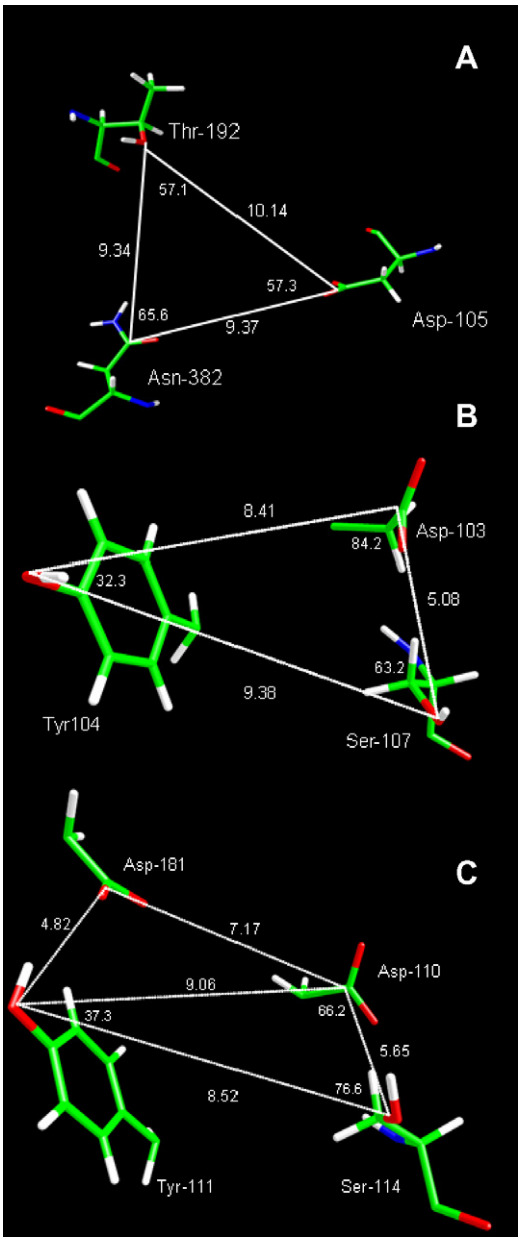

Figure 7. Geometric features of the arrangement of polar residues involved in agonists binding in M1 (A), M2 (B), and M5 (C).

When considering the hydrophobic residues which surround the bound agonists, the muscarinic binding sites can be divided in two clear-cut regions. The first subpocket interacts with ammonium head and is lined by aromatic residues which realize charge transfer interactions plus hydrophobic contacts, whereas the second region accommodates the acetylcholine's ester group and includes both aromatic and aliphatic residues which contact ligand's alkyl chains. In all analyzed subtypes, the hydrophobic contacts play a key role in determining the ligand recognition but the two mentioned regions have different structural properties in each subtype.

The M_1 subtype shows a region interacting with ammonium head which is symmetric, since the aromatic residues uniformly surround the ammonium group, but sterically limited as demonstrated by poor affinity of

Table 3. Geometric features of considered muscarinic binding sites

Subtype	Volume (Å^3)	Triangle	Area of triangle (Å^2)	Subpocket ammonium	Subpocket ester
M_1	2594	Equilater	41.16	Small-symmetric	Stereoselective
M_2	977	Isosceles	20.10	Wide-stereoselective	Symmetric
M_5	1171	Isosceles (plus Asp181)	22.12	small-symmetric	Stereoselective

nortropane derivatives (**27–28**); conversely the region interacting with ester group is ampler but stereospecific since the alkyl groups have to contact Leu386 and Ala193 as demonstrated by the relevance of C2′ configuration in the oxathiolane derivatives.

Conversely, M_2 subtype shows an ampler subpocket which accommodates the ammonium head (as demonstrated by marked affinity of nortropane derivatives) but stereospecific since the alkyl groups must contact Trp99 and Tyr104 avoiding to clash against Pro437. The wider subpocket of M2 receptor finds an interesting confirmation in the recently proposed oxotremorine analogs where the replacement of the pyrrolidine ring with a piperidine moiety almost doubles the affinity at M_2 receptor.[34] The region accepting the ester moiety is as wide as that of M_1 subtype (as indicated by very similar affinities of xanomeline) but symmetric since it is uniformly lined by apolar residues as shown by irrelevant role of C2′ configuration in oxathiolanes.

Finally, the M_5 subtype shows subpockets with structural features very similar to those of M_1 subtype. Indeed, the site interacting with ligand ammonium head is sterically limited mainly due to the second aspartate residue which further occupies the subpocket but symmetric as evinced by modest variability in affinities of congeners. Again, the subpocket accommodating the ester group is asymmetric since the alkyl groups must successfully contact Trp455 and Phe202.

When considering the arrangements of both polar and hydrophobic residues, the described interaction schemes allow for differentiation of each considered subtype (as summarized in Table 3). Indeed: (1) the M_1 binding site is the amplest one, even possessing a region interacting with ammonium head sterically restricted and the second subpocket ample but asymmetric; (2) the M_2 binding site is clearly smaller even possessing a wider region accommodating the ammonium head, and (3) the M_5 binding site is globally as ample as M_2 cavity but the region accepting the ammonium head is sterically limited due to the presence of Asp181.

4. Conclusions

The homogeneity of docking results, the agreement with mutational analyses, and the relevant correlations between docking scores and biological affinities confirm the reliability of the here developed interaction patterns for the considered muscarinic subtypes. What is more, these results seem to suggest that it is possible to differentiate the muscarinic binding sites according to both realized interactions and steric requirements. Hopefully, these findings could be exploited to design subtype selective muscarinic agonists with an improved functional profile.

5. Computational details

5.1. Ligand dataset

The number of considered ligands was severely limited by the remarkable difficulty to find in the literature fully comparable binding data for muscarinic agonists (especially for M_5 subtype). The considered compounds are, indeed, those for which affinity values on cloned human muscarinic receptors expressed in CHO cells were available. In particular, the ligand dataset can be divided in two subsets: the first include a series of fourteen oxathiolane and dioxolane congeners[35,36] (**1–14**, Chart 1), while the latter subset includes markedly more heterogeneous (Chart 2) compounds comprising, among others, natural compounds (i.e., muscarine,[37] arecoline,[38] oxotremorine,[39] pilocarpine,[40] and aceclidine[41]), bicyclic derivatives (sabcomeline,[42] **27**, and **28**[43]), and alkynyl derivatives (oxotremorine-M,[39] **21**, and **22**[44]).

The molecules were built using VEGAZZ software[45,46] and after a preliminary energy minimization to discard high-energy intramolecular interactions, the overall geometry and the atomic charges were optimized using MOPAC6.0 (keywords: 'AM1', 'PRECISE', 'GEO-OK'). The conformational profile was explored by a MonteCarlo procedure which generated 1000 conformers by randomly rotating the rotors. All geometries so obtained were optimized and clustered according to similarity to discard redundant ones; in detail, two geometries were considered as non-redundant if they differed by more than 60 degrees in at least one torsion angle.

5.2. Docking analyses

The docking and scoring procedures involved extensive rigid-body sampling with the OpenEye Scientific Software package FRED.[47] Briefly, FRED exhaustively searches into a predefined docking site/box, scoring, and filtering each binding pose with respect to a shape-based scoring function followed by a more stringent matching search which accounts for lipophilic and electrostatic interactions. In detail, the docking analyses exploited the mAChRs models as generated in the previous study and the FRED-based sampling was performed in 10 Å side box around the bound acetylcholine. The docking results were preliminarily scored considering all score functions computed by Fred software and the study is, thereby, focused on ChemScore function,[48] which accounts for both polar and hydrophobic interactions, since it gave the best correlations with affinity values.

References and notes

1. Eglen, R. M. *Prog. Med. Chem.* **2005**, *43*, 105.
2. van Koppen, C. J.; Kaiser, B. *Pharmacol. Ther.* **2003**, *98*, 197.
3. Wess, J. *Trends Pharmacol. Sci.* **2003**, *24*, 414.
4. Wess, J. *Crit. Rev. Neurobiol.* **1996**, *10*, 69.
5. Felder, C. C. *FASEB J.* **1995**, *9*, 619.
6. Felder, C. C.; Bymaster, F. P.; Ward, J.; DeLapp, N. *J. Med. Chem.* **2000**, *43*, 4333.
7. Wess, J.; Liu, J.; Blüml, K.; Yun, J.; Schöneberg, T.; Blin, N. Molecular Mechanisms of Muscarinic Acetylcholine Receptor Function. In *Mol. Biol. Intell. Unit*; Wess, J., Ed.; R.G. Landes: Austin, TX, USA, 1995.
8. Kenakin, T. P. *Pharmacol. Rev.* **1996**, *48*, 413–463.
9. Hulme, E. C.; Curtis, C. A.; Page, K. M.; Jones, P. G. *Life Sci.* **1995**, *56*, 891–898.
10. Han, S. J.; Hamdan, F. F.; Kim, S. K.; Jacobson, K. A.; Bloodworth, L. M.; Li, B.; Wess, J. *J. Biol. Chem.* **2005**, *280*, 34849–34858.
11. Allman, K.; Page, K. M.; Curtis, C. A.; Hulme, E. C. *Mol. Pharmacol.* **2000**, *58*, 175–184.
12. Fanelli, F.; De Benedetti, P. G. *Chem. Rev.* **2005**, *105*, 3297–3351.
13. Evers, A.; Hessler, G.; Matter, H.; Klabunde, T. *J. Med. Chem.* **2005**, *48*, 5448–5465.
14. Pedretti, A.; Vistoli, G.; Marconi, C.; Testa, B. *Chem. Biodivers* **2006**, *3*, 481–501.
15. Espinoza-Fonseca, L. M.; Pedretti, A.; Vistoli, G. *Arch. Biochem. Biophys.* **2008**, *469*, 142–150.
16. Bluml, K.; Mutschler, E.; Wess, J. *J. Biol. Chem.* **1994**, *269*, 18870.
17. Lu, Z. L.; Saldanha, J. W.; Hulme, E. C. *J. Biol. Chem.* **2001**, *276*, 34098.
18. Ward, S. D.; Curtis, C. A.; Hulme, E. C. *Mol. Pharmacol.* **1999**, *56*, 1031.
19. Hulme, E. C.; Lu, Z. L. *J. Physiol. Paris* **1998**, *92*, 269.
20. Peng, J. Y.; Vaidehi, N.; Hall, S. E.; Goddard, W. A., 3rd *ChemMedChem* **2006**, *1*, 878.
21. Hulme, E. C.; Lu, Z. L.; Saldanha, J. W.; Bee, M. S. *Biochem. Soc. Trans.* **2003**, *31*, 29–34.
22. Spalding, T. A.; Ma, J. N.; Ott, T. R.; Friberg, M.; Bajpai, A.; Bradley, S. R.; Davis, R. E.; Brann, M. R.; Burstein, E. S. *Mol. Pharmacol.* **2006**, *70*, 1974.
23. Allman, K.; Page, K. M.; Curtis, C. A.; Hulme, E. C. *Mol. Pharmacol.* **2000**, *58*, 175.
24. Schwarz, R. D.; Callahan, M. J.; Coughenour, L. L.; Dickerson, M. R.; Kinsora, J. J.; Lipinski, W. J.; Raby, C. A.; Spencer, C. J.; Tecle, H. *J. Pharmacol. Exp. Ther.* **1999**, *291*, 812.
25. Vogel, W. K.; Sheehan, D. M.; Schimerlik, M. I. *Mol. Pharmacol.* **1997**, *52*, 1087.
26. Heitz, F.; Holzwarth, J. A.; Gies, J. P.; Pruss, R. M.; Trumpp-Kallmeyer, S.; Hibert, M. F.; Guenet, C. *Eur. J. Pharmacol.* **1999**, *380*, 183.
27. Johren, K.; Höltje, H. D. *J. Comput. Aided Mol. Des.* **2002**, *16*, 795.
28. Niu, Y. Y.; Yang, L. M.; Liu, H. Z.; Cui, Y. Y.; Zhu, L.; Feng, J. M.; Yao, J. H.; Chen, H. Z.; Fan, B. T.; Chen, Z. N.; Lu, Y. *Bioorg. Med. Chem. Lett.* **2005**, *15*, 4814.
29. Piergentili, A.; Quaglia, W.; Giannella, M.; Del Bello, F.; Bruni, B.; Buccioni, M.; Carrieri, A.; Ciattini, S. *Bioorg. Med. Chem.* **2007**, *15*, 886.
30. Vistoli, G.; Pedretti, A.; Testa, B.; Matucci, R. *Arch. Biochem. Biophys.* **2007**, doi:10.1016/j.abb.2007.04.022.
31. Furukawa, H.; Hamada, T.; Hayashi, M. K.; Haga, T.; Muto, Y.; Hirota, H.; Yokoyama, S.; Nagasawa, K.; Ishiguro, M. *Mol. Pharmacol.* **2002**, *62*, 778.
32. Binkowski, T. A.; Naghibzadeh, S.; Liang, J. *Nucleic Acids Res.* **2003**, *31*, 3352.
33. http://sts.bioengr.uic.edu/castp/.
34. Dallanoce, C.; De Amici, M.; Barocelli, E.; Bertoni, S.; Roth, B. L.; Ernsberger, P.; De Micheli, C. *Bioorg. Med. Chem.* **2007**, *15*, 7626.
35. Dei, S.; Angeli, P.; Bellucci, C.; Buccioni, M.; Gualtieri, F.; Marucci, G.; Manetti, D.; Matucci, R.; Romanelli, M. N.; Scapecchi, S.; Teodori, E. *Biochem. Pharmacol.* **2005**, *69*, 1637.
36. Scapecchi, S.; Matucci, R.; Bellucci, C.; Buccioni, M.; Dei, S.; Guandalini, L.; Martelli, C.; Manetti, D.; Martini, E.; Marucci, G.; Nesi, M.; Romanelli, M. N.; Teodori, E.; Gualtieri, F. *J. Med. Chem.* **2006**, *49*, 1925.
37. De Amici, M.; Dallanoce, C.; De Micheli, C.; Grana, E.; Dondi, G.; Ladinsky, H.; Schiavi, G.; Zonta, F. *Chirality* **1992**, *4*, 230.
38. Kim, M. G.; Bodor, E. T.; Wang, C.; Harden, T. K.; Kohn, H. *J. Med. Chem.* **2003**, *46*, 2216.
39. Duttaroy, A.; Gomeza, J.; Gan, J. W.; Siddiqui, N.; Basile, A. S.; Harman, W. D.; Smith, P. L.; Felder, C. C.; Levey, A. I.; Wess, J. *Mol. Pharmacol.* **2002**, *62*, 1084.
40. Ward, S. D.; Curtis, C. A.; Hulme, E. C. *Mol. Pharmacol.* **1999**, *56*, 1031–1041.
41. Ehlert, F. J.; Griffin, M. T.; Glidden, P. F. *J. Pharmacol. Exp. Ther.* **1996**, *279*, 1335–1344.
42. Stengel, P. W.; Cohen, M. L. *J. Pharmacol. Exp. Ther.* **2001**, *296*, 818–824.
43. Daly, J. W.; Gupta, T. H.; Padgett, W. L.; Pei, X. F. *J. Med. Chem.* **2000**, *43*, 2514–2522.
44. De Amici, M.; Conti, P.; Fasoli, E.; Barocelli, E.; Ballabeni, V.; Bertoni, S.; Impicciatore, M.; Roth, B. L.; Ernsberger, P.; De Micheli, C. *Farmaco* **2003**, *58*, 739–748.
45. Pedretti, A.; Villa, L.; Vistoli, G. *J. Mol. Graph. Model* **2002**, *21*, 47–49.
46. VEGAZZ is downloadable at http://www.ddl.unimi.it.
47. http://www.eyesopen.com.
48. Eldridge, M.; Murray, C.; Auton, T.; Paolini, G.; Mee, R. *J. Comp.: Aided Mol. Des.* **1997**, *11*, 425–445.